

Validation of 3D Ultra-Short TE (UTE) Phase-Contrast MRI for Imaging of Steady Flow: Initial Phantom Experiments

Mo Kadbi¹, MJ Negahdar¹, Jung won Cha¹, Melanie Traughber²,
Peter Martin², and Amir A Amini¹

Abstract— Assessment of blood flow is an important factor in diagnosis of cardiovascular disease. Vascular stenosis result in disturbed blood flow, flow recirculation, turbulence, and flow jet. These types of flows cause erroneous quantification of blood flow using conventional Phase contrast (PC) MRI techniques. Previous investigations have revealed that shorter Echo Times (TE) can decrease the quantification errors. In this paper, we performed phantom studies under steady flow to validate the UTE technique. Investigation of three different constant flow rates revealed a significant improvement in flow quantification and reduction of flow artifacts in comparison to Cartesian Phase-Contrast MRI.

I. INTRODUCTION

Phase-contrast (PC) MRI is a powerful technique for quantitative measurement of blood flow in cardiovascular system. This technique has been employed for blood flow quantification in the heart [1-2], aorta and aortic valve [3-4], Carotid vessels [5-6], and various cardiovascular diseases. Vascular stenosis cause disturbed blood flow, flow recirculation, turbulence, flow fluctuation, and a jet distal to the narrowing. With conventional MR imaging techniques, these high velocities result in signal loss distal to the stenosis and cause miscalculation in flow quantification [7]. It has been shown in few studies that various factors can cause signal loss. Acceleration, higher order flow, and fluid mixing leading to intravoxel dephasing [8-9], and phase mis-registration errors due to phase shift between phase encoding steps [9-10] are the main reasons for signal loss. One important approach that results in significant impact in correction of the signal loss is reduction of the echo time (TE) and gradient duration. Several groups studied the effect of variation of TE on signal loss and velocity quantification [11-14]. Reducing the TE decreases the turbulent fluctuation velocity and intravoxel dephasing, resulting in higher signal to noise ratio and more reliable estimation of velocity in PC MRI. In [11], it was shown that the area of signal loss is increased by decreasing the pixel size and increased TE. Another study reported that by shortening the TE to 3.1 msec in MR angiography of Carotid arteries, the signal loss reduced [12]. However, even with TE=3.1 msec a significant dephasing and signal loss due to higher order motion and velocity fluctuation appeared.

In [13], the effect of TE and other parameters on signal loss was studied. By varying the TE between 2.7 and 19 msec, it was demonstrated that the least signal loss was achieved by TE=2.7 msec. Another study reported that a spiral phase-contrast sequence is capable of measuring flow in the case of high flow jet distal to stenosis [14]. The TE was reduced to 1.6 msec in this report but velocity quantification was still underestimated in comparison to Doppler. Recently, a new phase-contrast sequence based on the ultra-short TE (UTE) technique was presented with TE reduced to 0.65 msec [15]. This study proved to be a more reliable technique for measuring high velocities due to robustness to intravoxel dephasing and signal loss. However, this technique had some disadvantages including underestimation of low flow rates. In this paper, in phantom studies and under steady flow, we investigate a new 3D UTE PC MRI technique [16-17] with slightly longer TE compared to [15]. This method obviates the disadvantages of 2D UTE sequence. Flow assessment was carried out using an 87% area stenosis phantom under steady flow and comparison of accuracy of the 3D UTE technique with both spiral PC MRI and conventional PC MRI was also made. To evaluate robustness of the method, three steady flow rates were considered.

II. MATERIALS AND METHODS

A. Conventional (Cartesian) PC MRI

Phase Contrast MRI is based on phase differences of flowing spins compared to spins of stationary tissue. A flow sensitive and a flow compensated scan are acquired by applying a bipolar gradient in the flow direction of interest. Subsequently, an automatic complex subtraction of these scans is performed in order to measure the difference in phase of flowing spins – this phase difference is related to velocity. Figure 1(I) demonstrates a standard PC MRI sequences using the Cartesian trajectory. In this sequence, slice excitation and refocusing (a), flow encoding (b) and rephasing (c) gradients need to be applied during TE. These gradients (as long as TE) in Cartesian trajectory (TE is defined as the distance between the center of RF pulse to the center of readout window) prolong TE and may lead to phase errors and velocity miscalculations. K-space lines in Cartesian trajectory are acquired line by line with a constant sampling density throughout the k-space.

B. Spiral PC MRI

In spiral method instead of using horizontal lines in k- space, a spiral read-out trajectory is applied to cover the k-

Mo Kadbi, MJ Negahdar, Jung won Cha, and Amir Amini are with the Medical Imaging Lab, Dept. of Electrical and Computer Engineering, University of Louisville, Louisville, KY, United States. (e-mail: m0kadbi01@louisville.edu).

Melanie Traughber and Peter Martin are with Philips Medical System, Philips Healthcare, Cleveland, OH, USA 44143.

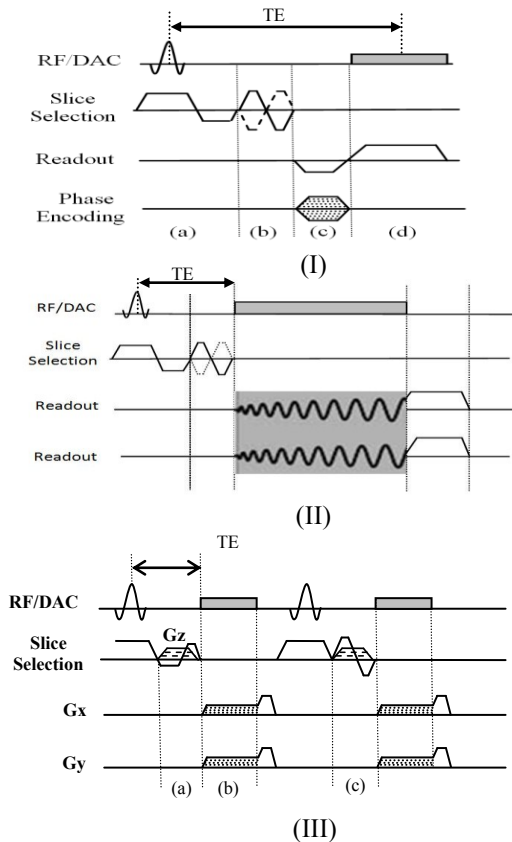


Figure 1. Cartesian (I), single-shot spiral (II), and 3D UTE (III) PC MRI sequences. G_x and G_y in 3D UTE show the radial readout gradients. III.a shows flow encoding gradient as well as slice encoding gradient G_z for 3D acquisition. III.b shows radial readout gradient in x and y direction and III.c shows flow compensated gradient in second scan.

space. In this method, the repetition time TR and total scan time can decrease significantly. The single shot spiral acquisition technique covers the entire k-space in one readout causing longer TR. Figure 1(II) demonstrates a single shot spiral PC MRI which spiral readout gradient in x and y direction cover the whole k-space in one TR. Single-shot spiral suffers from severe artifacts due to off-resonance. Multi-shot or interleaved spiral acquires multiple spiral shots in each TR. As a result, the whole k-space is collected using multiple but shorter spirals. This leads to reduction of off-resonance artifact.

C. 3D UTE PC MRI

Figure 1(III) shows the proposed 3D UTE-PC sequence [16-17] diagram where two back-to-back RF pulses and readout gradients are used in order to construct one flow sensitive image and one flow compensated (reference) image in the slice-select direction. The slice refocusing section of slice excitation gradient is combined with flow encoding (a) / compensation gradient (c) which results in shorter TE. TE is defined in this case as the distance between the center of the RF pulse to the beginning of the readout gradient. Sampling the k-space is started at the rising slope of readout gradient (b). The radial readout trajectory in 3-D UTE is based on radial traversal of evenly spaced k-space lines starting from center of k-space and ending on the surface of cylinder with radius K_{max} determined by spatial resolution in the in-plane

direction. A 3D non-cartesian trajectories acquisition based on “stack-of-stars” [18] strategy is employed to collect multiple slices in a cylindrical volume in flow encoding direction. The minimum TE for $V_{enc}=500$ and slice thickness 4 mm is 0.95 msec which is much shorter than Cartesian and spiral trajectories.

D. Experimental setup

An idealized rigid model of axisymmetric Gaussian shape was machined from transparent acrylic. We initially aimed the occlusion to have a 90% area narrowing at the throat. However, later, the exact geometry was measured with high-resolution CT ($0.22 \times 0.22 \times 0.625$ mm³) and the narrowing was determined to be 87%. There were additional imperfections in fabrication of the phantom which caused the phantom geometry to not be entirely axis-symmetric. The stenosis diameter is 25.4 mm at the inlet and narrows down to 9.04 mm at the throat. To ensure fully developed laminar flow, devoid of disturbance, at the entrance of the model, a 75-cm long straight rigid acrylic tube was positioned upstream of the phantom. Fluid viscosity was 0.0043 Pa.s and fluid density was 1060 kg/m³ at 65 deg. F. Figure 2 shows the stenotic phantom setup in a closed loop flow system. A CardioFlow 1000 programmable pump (Shelley Medical Imaging Technologies, London, Ontario, Canada) was used for generating steady flows.

Three flow rates indicating low ($Q=13.2$ mL/s), medium ($Q=39.4$ mL/s), and high ($Q=300$ mL/s) flow rate were studied. These flow rates translate to the following Reynolds numbers at the inlet: $Re = 160$, $Re = 480$, $Re = 3618$, and the following Reynolds numbers at the throat: $Re = 440$, $Re = 1324$, $Re = 10022$, respectively.

E. Imaging Protocol

Imaging was performed on an Achieva 1.5T Philips scanner using a 16-element SENSE knee coil. The imaging volume covered ~ 50 mm of phantom and the scan was repeated 6 times to covers 300 mm of phantom including 50 mm proximal and 250 mm distal to the center of the stenosis. Each scan included 17 slices for Cartesian and spiral trajectories with the slice thickness of 4 mm and 1 mm overlap between slices and 10 slices for 3D UTE sequence with the slice thickness of 4 mm and no overlap between slices. The imaging volume for 3D UTE is 40 mm along z

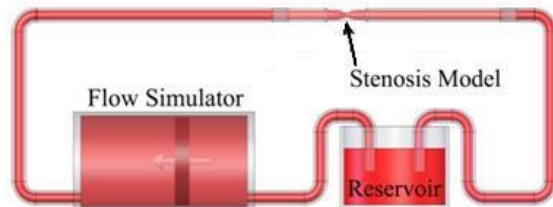


Figure 2. Schematic of the experimental setup showing the test section with 87% area stenosis which was machined in-house from clear acrylic plastic.

and the iso-center slice corresponds to the iso-center slices in Cartesian and spiral sequences. For the spiral trajectory, 30 interleaves each with 4ms readouts were used. The other parameters at Q=300 ml/s for Cartesian, spiral, and 3D UTE PC MRI are shown in table I.

III. RESULTS AND DISCUSSIONS

Figure 3 displays the magnitude image as well as the flow and velocity profiles for flow rate of Q=13.2ml/s 33mm distal to throat of the stenosis for cartesian, spiral and 3D UTE PC MRI. No signal loss appears in the magnitude image and velocity profiles have identical shapes. In order to compare the proposed 3-D UTE-PC MRI technique with conventional PC MRI and spiral sequences, the normalized mean square error (MSE) is calculated. The normalized root mean square error can be expressed as:

$$\text{Error} = \sqrt{\frac{1}{N} \left(\frac{Q_{\text{conv}} - Q_{\text{UTE}}}{Q_{\text{conv}}} \right)^2}$$

where Q_{conv} and Q_{UTE} describe measured flow using Conventional PC MRI and 3-D UTE-PC MRI technique respectively and N is the number of slices used for error measurement. The error for measured flow in low flow rate is shown in table II and Cartesian trajectory has the least error. Although spiral and 3D UTE reveal more errors compared to Cartesian, the accuracy of these techniques is reasonable. It is worth pointing out that the 3D UTE sequences shows significant improvement in low flow rates - decreasing the error to ~ 5%; a previously proposed 2D UTE sequence was reported to have ~ 27% error at Q=100 mL/s with an average velocity of 44 cm/s at Re=7200 [15]. This

TABLE I. ACQUISITION PARAMETERS AT Q=13.2,39.4, AND 300 ML/S FOR CARTESIAN, SPIRAL, AND 3D UTE PC MRI FOR PHANTOM STUDIES. THE CARTESIAN AND THE SPIRAL ACQUISITIONS WERE MULTI-SLICE 2-D ACQUISITIONS

Parameter	Cartesian PC MRI	Spiral PC MRI	3-D UTE-PC MRI
FOV [mm]	120x120x51	120x120x51	120x120x40
TE in Q=13.2 (ms)	5	3.5	2.5
TR in Q=13.2 (ms)	7.9	9.9	12.7
TE in Q=39.4 (ms)	4.4	2.9	1.9
TR in Q=39.4 (ms)	7.3	9.3	8.6
TE in Q=300 (ms)	4.2	2.5	0.95
TR in Q=300 (ms)	7.3	8.8	5.7
Venc at Q=13.2, 39.4, 300 (mL/s)	30, 75, 500	30, 75, 500	30, 75, 500
Spatial resolution(mm)	1.5x1.5x4.0	1.5x1.5x4.0	1.5x1.5x4.0
Flip angle (deg.)	12	12	12
Imaging time for one FOV (min)	3: 07	1:59	2:36

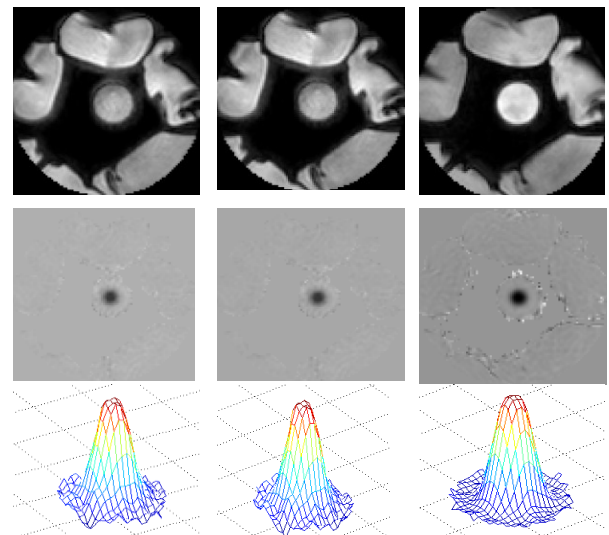


Figure 3. Magnitude image (first row), velocity image (second row), and velocity profile (third row) for low flow rate Q=13.2 mL/s at 33 mm distal to throat of the stenosis using Cartesian (first column), spiral (second column), and 3D UTE (third column) PC MRI sequences. The magnitudes, flows, and velocity profiles are in agreement. Note that in the first row, the cross section of the phantom is circular. Saline bags were placed around the phantom to permit the system to determine the resonance frequency.

improvement is likely due to the phase correction step as well as less phase error due to eddy current in our 3D UTE technique [16-17].

Figure 4 displays the measured flow and peak velocity for the three sequences and at three flow rates along the length of the phantom. The calculated flow rates along the length of the phantom for low and medium flow rates using three sequences are in good agreement and the errors for the non-Cartesian sequences (shown in table II) are acceptable. In case of low and medium flow rates, the measured flow rate using Cartesian trajectory had the most accuracy compared to the generated flow rate. However, the variability of peak velocity measured for the Cartesian sequence was higher than the other two techniques.

As previously reported [19], the measured flow using the Cartesian trajectory at high flow rates exhibits significant underestimation. This can also be seen in figure 4(III) where

TABLE II. AVERAGE FLOW RATE MEASURED THROUGH THE PHANTOM (AVERAGED OVER 85 SLICES - 25 CM OF LENGTH ALONG THE PHANTOM) - 5 CM PROXIMAL TO THROAT TO 20 CM DISTAL TO THROAT

	Low flow 13.2 mL/s		Medium flow 39.4 mL/s		High flow 300 mL/s	
	Flow	Error (%)	Flow	Error (%)	Flow	Error (%)
Cartesian	13.3	1	39.29	0.3	235.09	21.6
Spiral	12.61	4.5	36.55	7.2	254.62	15.1
3D UTE	13.91	5.3	40.55	2.8	305.99	2

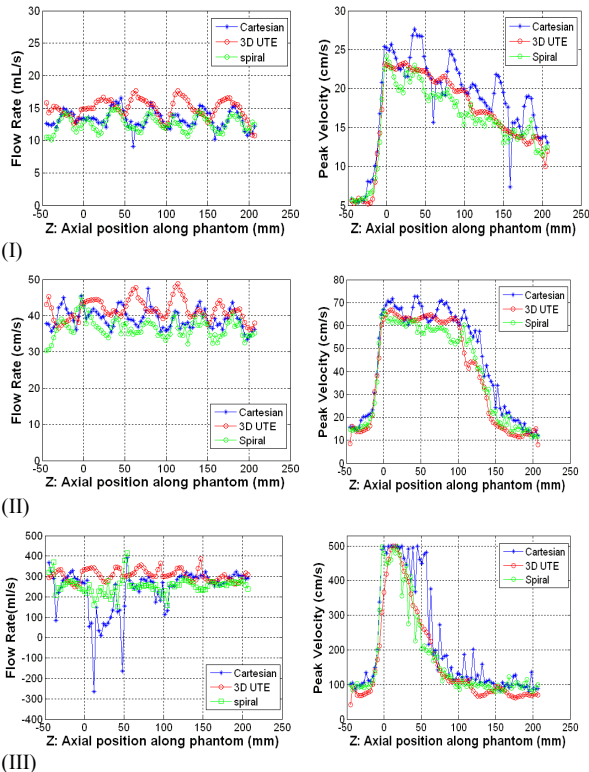


Figure 4. Measured flow rate (left column) and peak velocity (right column) for Cartesian, spiral and 3D UTE PC MRI sequences for low flow rate $Q=13.2$ mL/s along the length of the phantom (I), medium flow rate $Q=39.4$ mL/s (II), and high flow rate $Q=300$ mL/s (III). $Z=0$ denotes throat of the stenosis and $Z > 0$ correspond to positions downstream of the stenosis.

measured flow and peak velocity using Cartesian trajectory at $Q=300$ ml/s exhibits significant errors distal to the throat of the stenosis where a flow jet is present. Although the spiral PC sequence revealed less flow rate error and also less variability in the estimated peak velocity compared to the Cartesian trajectory, the most accurate measurements were obtained with the 3D UTE sequence.

Figure 5 displays the phantom magnitude and velocity image as well as velocity profile at high flow rate $Q=300$ mL/s. The magnitude image using Cartesian trajectory reveals a high signal loss while the corresponding velocity image shows significant phase error and noise at the center of jet due to the signal loss in magnitude image. Far less signal loss in magnitude image and phase error in velocity image can be seen in the spiral trajectory. This is because the shorter TE in the spiral sequence results in less intravoxel dephasing. In addition, spiral readout gradients oscillate periodically around zero and cause less intravoxel dephasing [20]. It should be noted however that the TE in spiral acquisition is not short enough to entirely resolve the signal loss and phase error. On the other hand, the 3D UTE sequence with significantly shorter TE, demonstrates no signal loss in the magnitude image and additionally, no phase error can be observed in the velocity image at the center of flow jet. The same phenomenon can also be seen in the corresponding velocity profiles. Note that the phase error in velocity image around the phantom is due to susceptibility artifact between

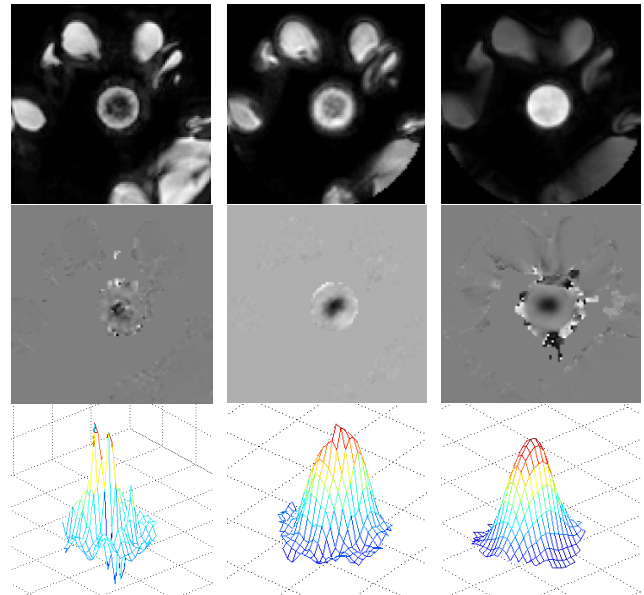


Figure 5. Magnitude image (first row), velocity image (second row), and velocity profile (third row) for high flow rate $Q=300$ mL/s at 33 mm distal to throat of the stenosis for the case of Cartesian (first column), spiral (second column), and 3D UTE (third column) acquisitions. The magnitudes images for Cartesian and spiral sequences show signal loss. The velocity image in the Cartesian acquisition reveals a significant phase error at the center of jet compared to spiral and 3D UTE. There is negligible signal loss and phase error in 3D UTE PC MRI.

phantom wall and surrounding air does not affect the flow measurement.

IV. CONCLUSIONS

In this paper, we reported on stenotic phantom experiments with steady flows and studied the accuracy of flow measurement with different k-space trajectories and echo times. A novel 3D UTE PC MRI technique [16-17] was compared with the conventional Cartesian PC MRI technique as well as with our group's previously published spiral PC MRI method [21]. With reduced TE, the spiral acquisition resulted in reduced signal loss and phase error in the magnitude and the velocity image. However, in comparison to the 3D UTE acquisition, a slight signal loss in the magnitude was still observable in the high flow rate $Q=300$ ml/s study. 3D UTE PC MRI resolved the signal loss and phase error entirely in the setting of high flow rate. In contrast with previously published 2D UTE sequence [19], the proposed 3D UTE PC MRI sequence shows less error in the setting of low flow and performs reliable flow assessment distal to the stenosis.

V. ACKNOWLEDGMENTS

This work was supported in part by the National Science Foundation under Grant 0730467 and by an innovative grant from the Clinical and Translational Research Program of the University of Louisville to A. Amini. We would like to thank M. Shakeri and I. Khodarahmi for providing Figure 2 in this paper.

VI. REFERENCES

- [1] A. Bolger, E. Heiberg, M. Karlsson, L. Wigstrom, J. Engvall, A. Sigfridsson, T. Ebbers, J. Kvitting, C. Carlhall, B. Wranne, "Transit of blood flow through the human left ventricle mapped by cardiovascular magnetic resonance," *J Cardiovasc Magn Reson*, 9:741–747, 2007.
- [2] P. Kilner, G. Yang, A. Wilkes, R. Mohiaddin, D. Firmin, M. Yacoub, "Asymmetric redirection of flow through the heart," *Nature*, 404: 759–761, 2000.
- [3] J. Kvitting, T. Ebbers, L. Wigstrom, J. Engvall, C. Olin, A. Bolger, "Flow patterns in the aortic root and the aorta studied with time-resolved, 3-dimensional, phase-contrast magnetic resonance imaging: implications for aortic valve-sparing surgery," *J Thorac Cardiovasc Surg*, 127:1602–1607, 2004.
- [4] M. Markl, M. Draney, M. Hope, J. Levin, F. Chan, M. Alley, N. Pelc, R. Herfkens, "Time-resolved 3-dimensional velocity mapping in the thoracic aorta: visualization of 3-directional blood flow patterns in Simulation of Phase Contrast MRI of Turbulent Flow 1045 healthy volunteers and patients," *J Comput Assist Tomogr*, 28: 459, 2004.
- [5] R. Vanninen, K. Koivisto, H. Tulla, H. Manninen, K. Partanen, "Hemodynamic effects of carotid endarterectomy by magnetic resonance flow quantification," *Stroke*, 26:84–89, 1995.
- [6] R. L. Vanninen, H. I. Manninen, K. P. Partane, P. A. Vainio, S. Soimakallio, "Carotid artery stenosis: clinical efficacy of MR phase-contrast flow quantification as an adjunct to MR angiography," *Radiology*, 194:459–467, 1995.
- [7] A. J. Evans, R. A. Blinder, R. J. Herfkens, et al, "Effects of turbulence on signal intensity in gradient echo images," *Invest Radiol*, 23:512-518, 1988.
- [8] J. N. Oshinski, D. N. Ku, R. I. Pettigrew, "Turbulent fluctuation velocity: the most significant determinant of signal loss in stenotic vessels," *Magn. Reson. Med*, 33, 193-199, 1995.
- [9] J. C. Gatenby, T. R. McCauley, J. C. Gore, "Mechanisms of signal loss in MR imaging of stenoses," in *Proc SMRM, 11th Annual Meeting, 1992.*, p. 2814.
- [10] R. L. Wolf, D. B. Richardson, C. C. LaPlante, J. Huston, S. J. Riederer, R. L. Ehman, "Blood flow imaging through detection of temporal variations in magnetization," *Radiology*, 185, 559-567, 1993.
- [11] R. P. Spielmann, O. Schneider, F. Thiele, M. Heller, E. Bucheler, "Appearance of poststenotic jets in MRI: dependence on flow velocity and on imaging parameters," *Magn. Reson. Imaging*, 9, 67-72, 1991.
- [12] P. Schmalbrock, C. Yuan, D. W. Chakeres, I. Kohli, N. J. Pelc, "Volume MR angiography: methods to achieve very short echo times," *Radiology*, 175, 861-865, 1990.
- [13] F. Stahlberg, L. Sondergaard, C. Thomsen, O. Henriksen, "Quantification of complex flow using MR phase imaging—a study of parameters influencing the phase/velocity relation," *Magn Reson Imaging*, 10:13–23, 1992.
- [14] K. S. Nayak, B. S. Hu, D. G. Nishimura, "Rapid quantitation of high-speed flow jets," *Magn Reson Med*, 50:366–372, 2003.
- [15] K. R. O'Brien, S. G. Myerson, B. R. Cowan, A. A. Young, and M. D. Robson, "Phase-contrast Ultrashort TE: a more reliable technique for measurement of high-velocity turbulent stenotic Jets," *Magn Reson Med*, 62(3):626-36, 2009.
- [16] M. Kadbi, H. Wang, M. Traughber, M. Alshaher, A. Yancey, J. Heidenreich, and A. A. Amini, "3D Cine Ultra-short TE (UTE) phase contrast imaging in carotid artery: comparison with conventional technique," *ISMRM 20th annual meeting & Exhibition, May 2012.*
- [17] M. Kadbi, H. Wang, M. J. Negahdar, L. Warner, M. Traughber, and A. A. Amini, "A Novel Phase-Corrected 3D Cine Ultra-Short TE (UTE) Phase-Contrast MRI Technique," *EMBC Annual Int. Conf. of the IEEE, 2012, submitted for publication.*
- [18] D. Peters, F. R. Korosec, T. M. Grist, W. F. Block, J. E. Holden, K. K. Vigen, C. A. Mistretta, "Undersampled projection reconstruction applied to MR angiography," *Magn Reson Med*, 43:91-101, 2000.
- [19] K. R. O'Brien, B. R. Cowan, M. Jain, R. A. Stewart, A. J. Kerr, A. A. Young, "MRI phase contrast velocity and flow errors in turbulent stenotic jets," *J Magn Reson Imaging*, 28:210–218, 2008.
- [20] C. H. Meyer, B. S. Hu, D. G. Nishimura, A. Macovski, "Fast spiral coronary artery imaging," *Magn Reson Med.*, 28(2):202-13, Dec. 1992.
- [21] M. J. Negahdar, M. Kadbi, M. Kotys, M. Alshaher, S. Fischer, A. A. Amini, "Rapid flow quantification in iliac arteries with spiral phase-contrast MRI," *EMBC Annual Int. Conf. of the IEEE*, pp.2804-2808, Aug. 2011.